Research Article GU J Sci 36(1): 383-397 (2023) DOI: 10.35378/gujs.1012201

Gazi University

Journal of Science

http://dergipark.gov.tr/gujs

Numerical Analysis of Hydraulic and Thermal Performance of Al_2O_3-Water Nanofluid in a Zigzag Channel with Central Winglets

Selma AKCAY *

Cankiri Karatekin University, Mechanical Engineering Department, 18100, Cankiri, Turkey

Highlights

- The effects of winglets and nanofluids on the thermal performance in a zigzag channel are examined.
- The results are given in terms of thermal performance and friction factor.
- The heat transfer improves with increasing *Re* and φ, but the friction factor increases slightly.
- The temperature and velocity contours are presented for the zigzag channel with/without winglet.

Article Info

Received: 19 Oct 2021
Accepted: 01 Feb 2022

Keywords

Zigzag channel
Central winglet
Nanofluid
Heat transfer
Friction factor

Abstract

This study numerically examined the impacts of central winglets and Al_2O_3-water nanofluid on the thermo-hydraulic performance in a zigzag channel. The analyzes based on Computational Fluid Dynamic (CFD) using the SIMPLE algorithm are actualized for nanofluid flow in Reynolds numbers (*Re*) varying between 200 and 1200. The volume fraction of nanoparticle (φ) is changed from 1% to 5 %. The upper and lower zigzag surfaces are kept at T_w = 350 K constant temperature. The results are given in terms of thermal improvement (η), dimensionless friction factor (Γ), and thermo-hydraulic performance (*THP*). In addition, the work is compared with the zigzag channel without winglet for the base fluid. The temperature and velocity distributions are obtained for the zigzag channel with and without winglet at different Reynolds numbers. The results show that the nanofluid and winglets contribute considerably to the enhancement of heat transfer, but the friction factor slightly increases. The heat transfer improves with increasing inlet velocity and particle volume fraction. The highest thermo-hydraulic performance is obtained as approximately 2.12 for *Re* = 400 and φ = 0.05.

1. INTRODUCTION

In engineering applications, heat transfer improvement is an important research area as it contributes to the efficiency of thermal devices. Passive methods are often used to increase heat transfer without reducing the overall efficiency of these devices. These methods are applications such as in channel baffles, fins, winglets, vortex generators and corrugated channel geometries in different configurations. These applications are preferred in refrigeration and air conditioning systems, transportation, nuclear reactors, heat exchangers, solar air heaters, chemical or food processing such as many applications. This method is economical and reliable compared to other techniques as it does not involve dynamic motion and does not require external power [1-6].

Corrugated channels are preferred in many engineering applications. These surfaces both increase surface area and cause self-flow oscillation. Thus, these channels have an important role in increasing thermal efficiency. This improvement substantially depends on the channel geometrical properties [7-12]. Several passive methods are used simultaneously to further improve thermal performance. Extended surfaces such as fins/baffles are generally preferred to increase the heat transfer area. Many researchers examined the flow and thermal characteristic in channel with different configurations of the baffles [13-18]. Promvonge *et al*. [19] experimentally examined thermal performance in a channel where inclined horseshoe baffles were used. They declared that the heat transfer increased by approximately 92-208% and the pressure drop increased by 1.76-6.37 compared to straight channels. Kumar *et al.* [20] carried out an experimental study

*e-mail: selmaakcay@karatekin.edu.tr

to investigate the heat transfer effectiveness of the solar air duct using multiple V-type baffles. Sahel *et al.* [21] informed that the different baffle design in a rectangular channel improved thermal performance by 65%. Menni *et al.* [22] conducted a numerical study to examine the hydraulic and thermal performance of two 'S'-shaped baffles in different directions ('S'-upstream and 'S'-downstream) placed in the solar air duct. They reported that the heat transfer rate substantially increased based on the S-baffle arrangement and the flow velocity, and the highest thermal enhancement was found around 1.513 at Re = 32000 and S-downstream. Luan and Phu [23] suggested correlations for hydraulic and thermal behavior of an air heater duct including curved baffles. Bensaci *et al.* [24] realized an experimental and numerical study to research thermo-hydraulic effectiveness of air heaters with different baffle positions. The results shown that the highest thermal effectiveness was obtained when the baffles were placed in the first half of the duct. Wang *et al.* [25] studied the effects on heat transfer of factors such as different rib parameters, radiation intensity, mass flow rate in the solar air heater. They reported that the thermal performance of the duct with S-shaped rib increased up to 48% compared to the straight duct.

Another passive technique used to enhance thermal performance is the use of vortex generators within the channel. Vortex generators are applications that help generate longitudinal vortexes in the flow and help reduce thermal resistance by improving flow mixing. It has been reported that very high heat transfer improvement has been achieved in studies on this subject, and therefore, these studies have been the focus of high interest in recent years [26-31]. Modi and Rathod [32] presented a numerical study to examine the effects of vortex generator with several configurations on hydraulic and thermal behaviors in the wavy channels within certain range of the Reynolds number ($400 \leq Re \leq 1000$). They declared that vortex shapes significantly affect the hydraulic structure and thermal behaviors. Promvonge *et al.* [33] experimentally and numerically investigated the thermal effectiveness at under effects of turbulence regime ($4200 \leq Re \leq 25800$) in a heat exchanger with discrete V winglets. The effects on the heat transfer and the pressure drop of parameters such as different winglet-pitches and winglet heights at two different arrangements of V winglets (upstream and downstream) were investigated. The results reported that at a specific winglet height, the smallest pitch length ensured the highest Nusselt number and pressure drop.

On the other hand, fluids containing water, ethylene glycol, and oil widely used in industrial applications, have low thermal properties. New technologies are used to enhance the thermal characteristics of such conventional coolants. One of these techniques is to use nanoparticles to increase the thermal conductivity of the basic fluid. Some researchers have used nanofluids together with other passive techniques [34-40]. Manca *et al*. [41] studied the hydraulic and thermal characteristics for the $20000 \leq Re \leq 60000$ of Al_2O_3-water nanofluid at different rib heights, at 0% to 4% nanoparticle volume ratios in a channel. As a result, they reported that as Re and particle volume ratio increased, the heat transfer improved and at the same time an increase was observed in the pumping power. Heshmati *et al*. [42] numerically studied the mixed convective at $50 \leq Re \leq 400$ with the baffles of different geometries at varying particle volume ratios ($0.01 \leq \phi \leq 0.04$) of different nanofluids. It was reported that nanofluids with high particle volume ratios and small particle diameter significantly improve heat transfer. Huminic and Huminic [43] presented a review study on hydraulic and thermal behavior of basic fluids and nanofluids in the corrugated channel. Menni *et al.* [44] carried out the dynamic and thermal behavior of nanofluids in turbulent flow conditions by using baffles at different angles in the channel and reported that the highest thermal improvement was obtained when vertical baffles were used at high Reynolds numbers. Qi *et al.* [45] numerically and experimentally researched the flow and heat transfer behavior of nanofluids (TiO_2-water) in a wavy channel. Pordanjani *et al*. [46] carried out a review study examining the effects of nanofluid applications on energy savings in heat exchangers. Mei *et al.* [47] numerically investigated the flow and heat transfer of nanofluids (Fe_3O_4-water) using magnetic field in a wavy channel. Kaood and Hassan [48] numerically investigated the flow and heat transfer improvement and energy performance of different nanofluids in different wavy channel geometries. They reported that nanofluids were increased heat transfer according to smooth channel, and all performance improvement decreased at $Re \geq 10000$ for all fluids and channel configurations. The thermal, frictional and exergy behavior of triangular vortex generator in a channel with different cross-sectional areas were examined by Tian *et al.* [49]. In their study, air, water and two different nanofluids (Al_2O_3-water and CuO-water) were used. They declared that the most thermal effectiveness was obtained the circular cross section and the vortex generators enhanced significantly the Nusselt number when the nanofluids are employed as the working fluid. However, nanofluids caused more exergy destruction as well. Ajeel *et al.*

[50] numerically examined the hydraulic and thermal properties of nanofluids (ZnO-water) for turbulent flow with L-shaped baffles in a curved wavy channel and reported that the baffles and nanofluids have a considerable influence on increasing the heat transfer rate. Experimental investigations of convection heat transfer in a circular copper tube using graphene oxide nanofluid carried out by Karabulut *et al*. [51-53] and Kilinc *et at.* [54]. The results of their study reported that nanofluids improved heat transfer by about 48%.

As seen from previous studies, the baffles/winglets added to the channel increase the thermal performance. Even if the thermal performance using baffle/winglet is improved, the friction factor increases due to the reduced flow area. Thus, it is quite difficult to determine the benefit of both the fin/baffle/winglet regulations and the channel geometries, and a definite criterion has not been reported for determining optimum fin/baffle/winglet shapes and corrugated channel geometries in the literature works. There are many experimental and numerical studies investigating the combined impact of passive heat transfer applications. However, the high number of parameters examined increases the efforts to find the optimum parameters and as demonstrated above, further studies on nanofluid flow in corrugated channel with baffles/winglets needed. In the literature studies, winglets with different configurations have been used in straight channels. The effect of central winglets in a channel with the specified geometry was not investigated. In the presented study, the effects of both corrugated channel geometry and central winglets on the nanofluid flow and heat transfer were investigated together. Therefore, in this study, unlike other works, the different zigzag corrugated channel geometry (consisting of expanding modules) with central winglets were considered. The effects on hydraulic and thermal performance of Al_2O_3-water nanofluid for different particle volume fractions ($0.01 \leq \varphi \leq 0.05$) under laminar flow conditions ($200 \leq Re \leq 1200$) in this channel were numerically examined.

2. NUMERICAL STUDY

2.1. Numerical Model

In Figure 1, the geometry of the zigzag channel with central winglets is given together with the winglet detail. The height of channel is considered as D = 19 mm. At the inlet and outlet of channel, there is an unheated flat section $L_1 = 6D$ and the total length of the zigzag channel is $L_2 = 9D$. The length of zigzag section is considered as $S = 1.5D$ and the thickness as $t = 0.2D$. The length of winglet is $a = 0.2D$, the winglet thickness is $b = 0.08D$ and the angle between winglets is $\alpha = 14$ degree. Other geometric parameters are kept constant in the study. Aluminium is considered as the channel material.

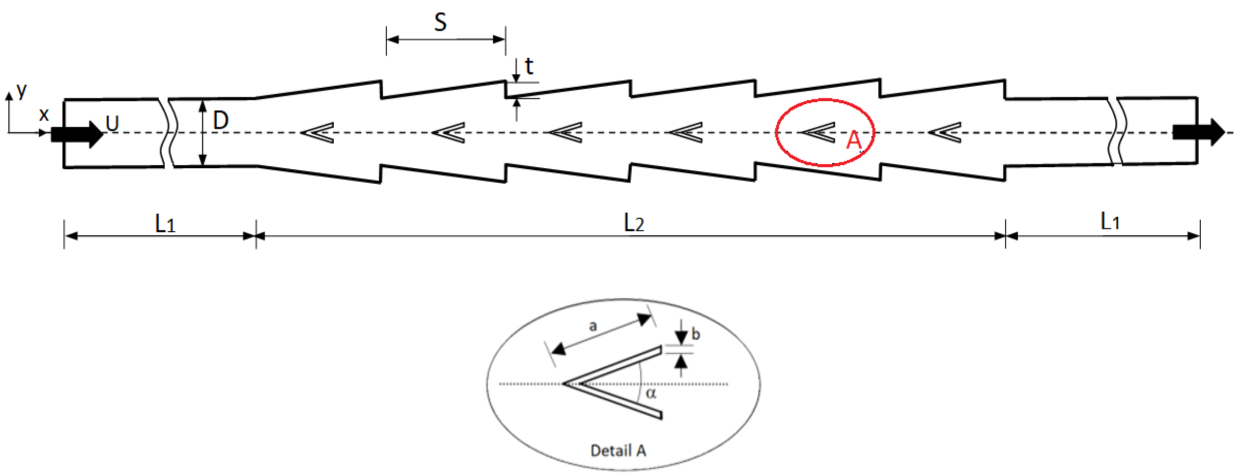

Figure 1. *The geometry of the numerical model with detail*

Al_2O_3-water suspension is considered as the nanofluid, and three different nanoparticle volume fractions (φ = 1%, 3% and 5%) are used. The simulations are applied under laminar flow conditions for $200 \leq Re \leq 1200$.

2.2. Numerical Procedure and Analysis

The numerical study is applied under the following supposition and the flow and the heat transfer are examined.

- Fluid is incompressible, single phase and Newtonian type
- The flow is steady, two-dimensional, laminar regime
- Fluid properties have not changed
- Gravity and viscous terms are neglected.
- Heat transfer with radiation is ignored.

According to the above acceptances assumptions, the governing equations are given in the cartesian tensor system as follows:

Continuity equation,

$$\nabla(\rho u) = 0, \tag{1}$$

Momentum equation:

$$\frac{\partial(u_i u_j)}{\partial x_i} = \frac{\partial p}{\partial x_i} + \frac{1}{\mathrm{Re}}\nabla^2 u_j, \tag{2}$$

Energy equation:

$$u_i \frac{\partial T}{\partial x_i} = \frac{1}{\mathrm{Re}\,\mathrm{Pr}}\nabla^2 T. \tag{3}$$

The numerical solutions are carried out with the Computational Fluid Dynamics (*CFD*) software-based FLUENT 15.0 program [55]. The simulations are solved with the SIMPLE algorithm and the terms convection and diffusion are discretized using a second order upwind scheme. The convergence criterion was taken as 10^{-6} for entire residuals.

The parameters relevant in this study are fluid velocity (Reynolds number, *Re*), particle volume fraction (φ), friction factor (f), thermal performance (Nusselt number, *Nu*) and thermo-hydraulic performance (*THP*). Several equations for this study are presented below:

The Reynolds number is written as

$$\mathrm{Re} = \frac{\rho u D_h}{\mu} \quad , \tag{4}$$

The local Nusselt number is calculated given by

$$Nu_x = \frac{h D_h}{k} \quad , \tag{5}$$

where ρ is the density, μ is the dynamic viscosity, D_h (= 4A/W) is the hydraulic diameter of the channel, k is the heat conductivity coefficient of the fluid.

$$q'' = h\Delta T_{lm} \tag{6}$$

$$\Delta T_{lm} = \frac{(T_i - T_o)}{\ln\left(\dfrac{T_w - T_i}{T_w - T_o}\right)} \tag{7}$$

where, q'' is heat flux, h is heat convective coefficient, ΔT_{lm} is logarithmic temperature difference.

The average Nusselt number is calculated along the channel length (L) as follows

$$Nu = \frac{1}{L}\int_0^L Nu_x dx \quad . \tag{8}$$

The heat transfer performance (η) calculated based on the Nusselt number is defined as

$$\eta = \frac{Nu_n}{Nu_o} \tag{9}$$

where Nu_n and Nu_o are Nusselt number for the nanofluids flow in the zigzag channel with winglets and Nusselt number for the base fluid (water) in the zigzag channel without winglet, respectively.

On the other hand, depending on the particle volume fraction and fluid velocity, a significant pressure drop occurs in the channel. Due to the high viscosity of nanofluids relative to the base fluid, friction factor should also be evaluated in heat transfer improvement studies.

The friction factor (f) is defined as

$$f = \frac{2\Delta P D_h}{\rho u^2 L} \tag{10}$$

where ΔP is the pressure difference at the inlet and outlet of the channel. Dimensionless friction factor is defined as

$$\Gamma = f_n / f_o \tag{11}$$

where f_n and f_o are friction factor for the nanofluids flow in the zigzag channel with winglets and friction factor for the base fluid (water) in the zigzag channel without winglet, respectively.

The thermo-hydraulic performance (THP) is calculated as follow

$$THP = \frac{(Nu_n / Nu_o)}{(f_n / f_o)^{1/3}} \quad . \tag{12}$$

Thermo-physical properties of nanofluids are calculated with the help of the following equations [44]

$$\rho_{nf} = (1-\varphi)\rho_{bf} + \varphi\rho_{pt} \tag{13}$$

$$c_{nf} = \frac{(1-\varphi)\rho_{bf}c_{bf} + \varphi\rho_p c_{pt}}{\rho_{nf}} \tag{14}$$

$$k_{nf} = k_{bf}\frac{\left[k_{pt} + 2k_{bf} - 2\varphi(k_{bf} - k_{pt})\right]}{\left[k_{pt} + 2k_{bf} + \varphi(k_{bf} - k_{pt})\right]} \tag{15}$$

$$\mu_{nf} = \mu_f (1 + 2.5\varphi \quad . \tag{16}$$

The water is used as the base fluid. Thermo-physical properties of water and Al_2O_3 nanoparticle are given in Table 1 [56].

Table 1. *Thermo-physical properties of water and Al_2O_3 nanoparticle*

	ρ [kg/m^3]	c [j/kgK]	k [W/mK]	μ [kg/ms]
water	998	4182	0.613	0.001003
Al_2O_3	3950	765	36	-

2.3. Boundary Conditions

The inlet temperature of fluid is T_i = 293 K. At the channel entrance, the "velocity inlet" boundary condition is applied. Fully developed flow is accepted at the outlet and "outflow" boundary condition is defined. The upper and lower zigzag surfaces are maintained at a constant temperature of T_w = 350 K and the winglets are defined adiabatic wall conditions. No-slip wall conditions are applied over the zigzag surfaces and the winglets. A non-slip and adiabatic boundary condition are applied for the straight section at inlet and outlet of the channel.

2.4. Grid Independence Test

In the study, the solutions for different grid numbers are compared and a grid-independent solution is obtained. After 106820 grid numbers, the difference between Nusselt numbers is determined to be less than 2%. Therefore, the mesh number of 106820 is adopted for the numerical model. Variation of mesh number and Nusselt number is given in Table 2 and Figure 2.

Table 2. *The results of grid independence test (basic fluid, with central winglets)*

Element Number	Nusselt Number (*Nu*)		
	Re = 200	*Re* = 600	*Re* = 1000
42624	3.725	11.245	18.455
75346	5.703	13.315	20.791
106820	6.049	14.012	21.087
137114	6.074	14.038	21.114
185793	6.078	14.041	21.116

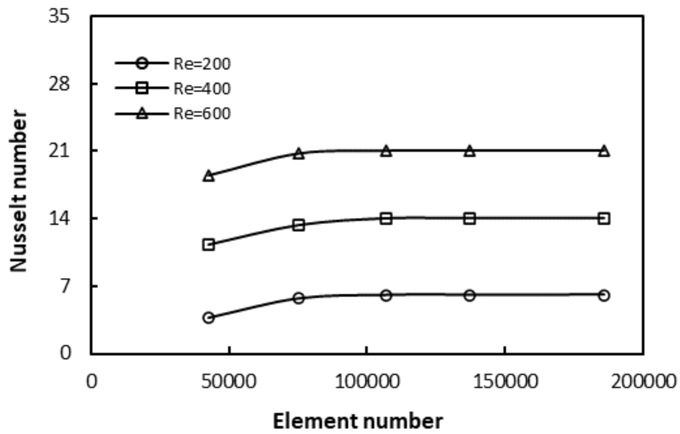

Figure 2. *The grid independence testing (basic fluid, with central winglets)*

Gambit program is used to prepare mesh structure of the numerical model. The mesh structure for the zigzag corrugated channel with central winglets is given in Figure 3.

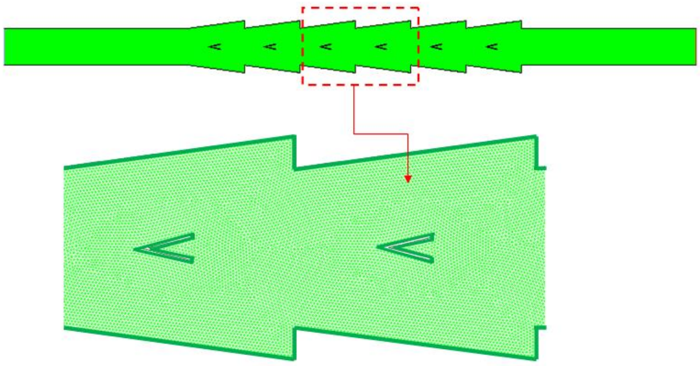

Figure 3. *The mesh structures of the numerical model with central winglets*

3. RESULTS AND DISCUSSION

For validity of the solutions, the numerical results of this study are compared with the experimental study conducted by Meyer and Abolarin [57]. A constant heat flux of q'' =2 kW was implemented to a flat channel surface (D_h = 19 mm) and heat transfer was calculated at x/D distances along the channel for Re = 1331. The agreement between the results of both studies is shown in Figure 4.

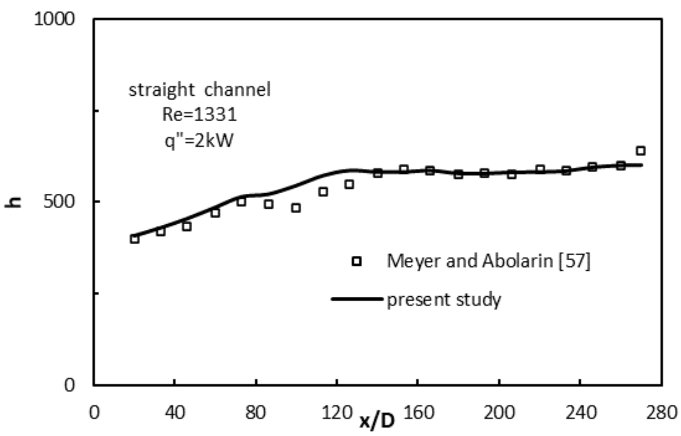

Figure 4. *Validity of the numerical solution*

In this section, the velocity, temperature and vorticity magnitude structures are obtained in the zigzag channel to explain the hydraulic and thermal mechanism. Figure 5 shows the velocity contours (a) and temperature distributions (b) for the base fluid in the zigzag channel without winglet at *Re* = 200 and *Re* = 1200. It is showed that the zigzag channel structure affects the flow and temperature fields depending on the Reynolds number. The fluid is directed towards the zigzag surfaces. A thinner velocity boundary layer is obtained with increasing flow velocity in the zigzag corrugated channel without winglet (Figure 5a). This case helps to reduce the thermal resistance and thus, the surface temperature of the channel decreases. Figure 5b indicates that the surface temperature of the channel is lower at Re=1200 than at Re=200.

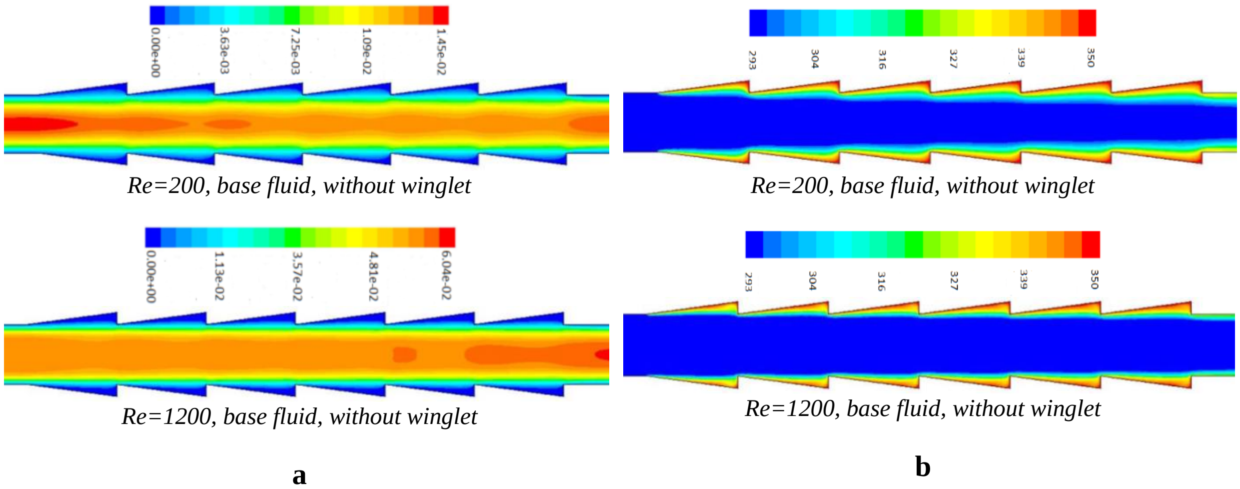

Figure 5. *For the base fluid in the zigzag channel without winglets at Re=200 and Re=1200 a) Velocity contours b) Temperature distributions*

Baffles/fins or winglets used to increase thermal performance in channel flows are placed in sequential or staggered array. After each baffle or winglet, the velocity and thermal boundary layer breaks down and these structures help create secondary flow loops. Disruption and reattachment of the flow after each baffle/winglet is reduces thermal resistance and increases the heat transfer rate. Therefore, in present study, central winglets were placed in the zigzag channel and the effects of these winglets on hydraulic and thermal behaviors were examined.

Figure 6a presents the velocity distributions at different *Re* for base fluid in the zigzag channel with central winglets. The winglets help the fluid to be directed towards the zigzag surfaces by separating the flow in to two branches.

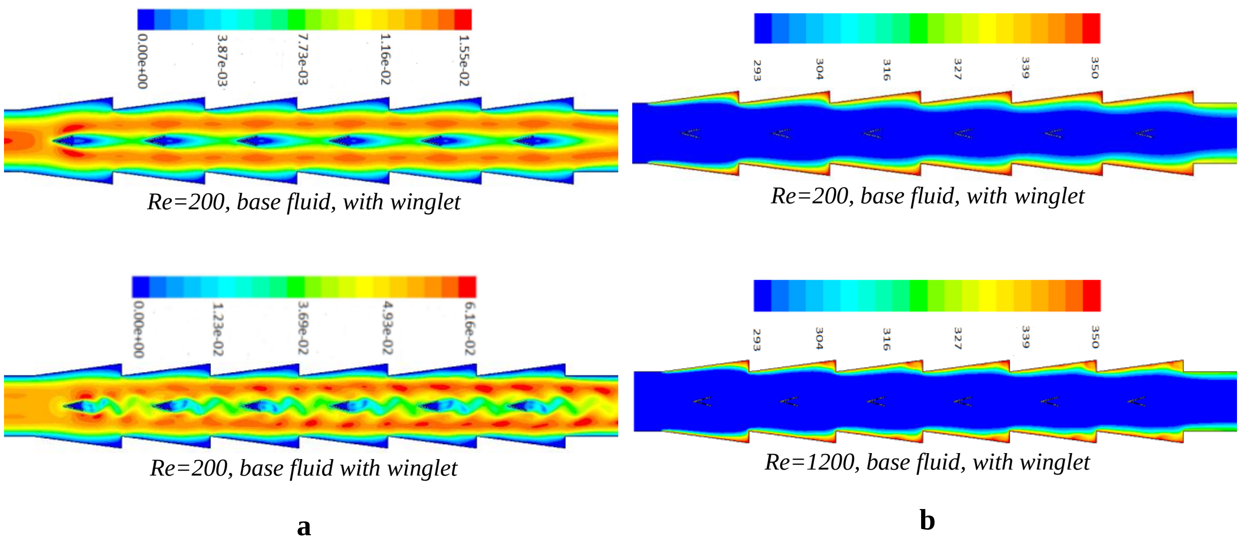

Figure 6. *For the base fluid in a zigzag channel with central winglets at Re = 200 and Re = 1200* a) *Velocity contours b) Temperature distributions*

Thus, the cold fluid contacted the hot surfaces better and this case is repeated after each winglet. Flow oscillation occurs in the channel with effect of the winglets. The flow oscillations behind of the winglets increase with Reynolds number. The change in the flow fields is also reflected in the temperature fields in the channel. The temperature contours are given for same parameters in Figure 6b. It is seen that for *Re* = 1200, the channel surface temperature is lower than *Re* = 200.

Figure 7 indicates the vorticity magnitude contours for the base fluid in the zigzag channel with and without winglet at *Re* = 200 and *Re* = 1200. It is seen that the central winglets in the zigzag channel substantially affect the vortex structures depending on Reynolds number. For the channel flow without winglet (Figure 7a), flow cycles occur only in the regions close to the zigzag channel surfaces. Increasing Reynolds number caused these flow cycles to grow downstream. In Figure 7b, the winglets placed in the center of the channel created secondary flow structures throughout the channel. At *Re* = 1200, these structures continued periodically both in the center and on the zigzag channel surfaces. These cycles help the laminar substrate to break down continuously, thereby reducing thermal resistance. Consequently, the rise in the heat transfer rate causes the channel surfaces to cool. Secondary flow structures and central vortex zones formed in the flow directly affect the temperature fields. Because these structures provide better mixing of the fluid in the wall surface and core region, it causes a high temperature gradient along the channel surfaces. These winglets placed in the center of the channel prove to have a major impact in heat transfer enhancement.

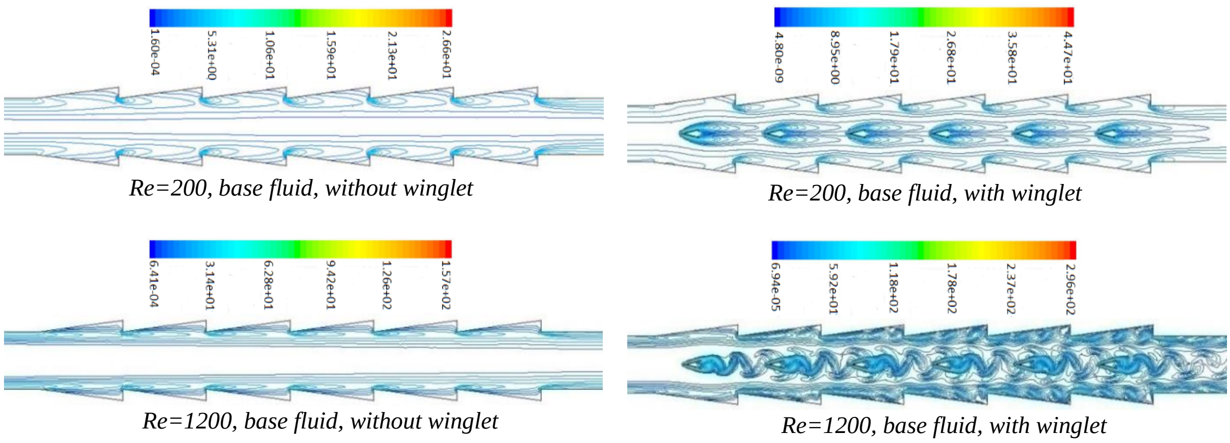

a **b**

Figure 7. *Vorticity magnitude contours for the base fluid in a zigzag channel at Re = 200 and Re = 1200 a) without winglet b) with winglets*

The variations of the thermal performance for different φ and *Re* in Figure 8a, the dimensionless friction factor in Figure 8b and the *THP* in Figure 8c are given by comparison the zigzag channel with and without winglet. The dashed line represents the base fluid flow for the zigzag channel without winglet. From the Figure 8a, it is visible that the heat transfer performance rises as the particle volume fraction rises compared to the channel without winglet. The heat transfer performance peaked at *Re* = 400 and tended to decrease slightly at later Reynolds numbers. Because the increase rate of the Nusselt number obtained for nanofluid flow in the zigzag channel with winglet has slightly decreased compared to the base flow in the channel without winglet. The highest heat transfer performance was found to be approximately Nu_n/Nu_o = 2.52 for *Re* = 400 and φ = 0.05. In the channel with central winglet for base fluid, the heat transfer performance improved by about 1.69 compared to the channel without winglet. Although heat transfer is increased with the addition of winglets, the pressure drop within the channel also increases due to the decreasing flow field effects. It can be visible in Figure 8b that the dimensionless friction factor increases as *Re* and φ increase compared to the channel without winglet. The highest friction factor was achieved to be approximately f_n/f_o = 1.72 for *Re* = 1200 and φ = 0.05. In the channel with central winglet for base fluid, the friction factor increased by about 1.43 compared to the channel without winglet. It can be said that the friction occurring in the channel are within acceptable limits.

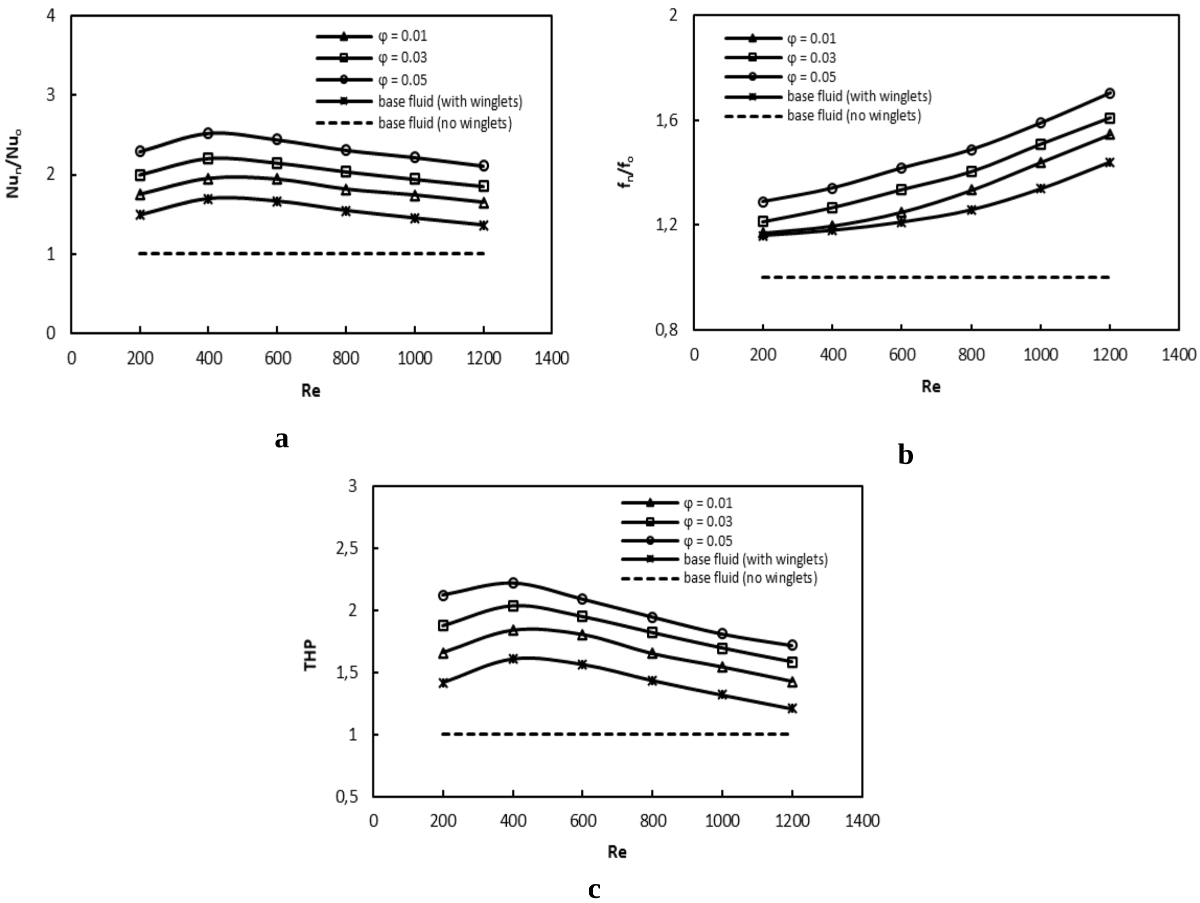

***Figure 8**. a) The heat transfer performance b) The dimensionless friction factor c) THP*

It can be observed from Figure 8c that the thermo-hydraulic performance rises with the particle volume fraction compared to the channel without winglet. Thermo hydraulic performance curves were obtained to be similar heat transfer performance curves. The *THP* curves are above the reference value for all parameters. Because the heat transfer performance is greater than the frictions in the channel. The curves peaking for Re = 400 showed a downward trend after *Re* > 400. This is because the friction factor increases more than the thermal improvement. The highest THP was obtained to be approximately 2.12 for *Re* = 400 and φ = 0.05. In the channel with central winglet for base fluid, the *THP* improved by about 1.61 according to the channel without winglet.

4. RESULTS

In present study, the thermal performance, friction factor and thermo-hydraulic performance of the nanofluids (Al_2O_3-water) flow in a zigzag channel with central winglet were investigated numerically. The effects of particle volume fraction and *Re* on the hydraulic and thermal behaviors were examined. The study was also compared with the base fluid the zigzag channel without winglet. The important numerical results are given by

- The velocity, temperature and vorticity contours were presented in the channel to understand hydraulic and thermal behaviors. The results of study indicated that the contours were highly influenced by channel geometry.
- There is significantly the effect of central winglets for thermal enhancement.
- In the channel with winglet, the thermal improvement is 1.69 times higher than in the channel without winglet.
- The dimensionless friction factor increased with *Re* and φ.
- Al_2O_3-water nanofluid in the zigzag channel with central winglet provided considerable improvement in heat transfer, while an acceptable increase in friction factor was seen.

- The highest thermal performance was obtained as 2.52 at *Re* = 400 and φ = 0.05.
- The highest dimensionless friction factor was found to be 1.72 at *Re* = 1200 and φ = 0.05.
- Thermo-hydraulic performance was achieved above the reference value for all parameters.
- The highest thermo-hydraulic performance was obtained as approximately 2.12 for *Re* = 400 and φ = 0.05.

NOMENCLATURE

A	cross sectional area (m^2)
a	winglet length (m)
b	winglet thickness (m)
D_h	hydraulic diameter (m)
f	friction factor
h	heat transfer coefficient (W/m^2K)
k	heat conduction coefficient (W/mK)
L	length of channel (m)
Nu	Nusselt number [$=hL/k$]
Pr	Prandtl number [$=\mu C_p/k$]
Re	Reynolds number [$=uD_h/v$]
S	length between winglets (m)
T	temperature (K)
THP	Thermo-hydraulic performance [$=Nu_n/Nu_o/(f_n/f_o)^{1/3}$]
u	average velocity (m/s)
W	wet circumference (m)
ΔP	pressure drop (Pa)
ΔT_{lm}	logarithmic temperature difference (K)

Greek symbols

α	winglet angle (degree)
η	heat transfer performance [$=Nu_n/Nu_o$]
μ	dynamic viscosity (Pa/s)
ρ	density of fluid (kg/m^3)
υ	kinematic viscosity (m^2/s)
φ	nanoparticle volume fraction (%)
Γ	dimensionless friction factor [$=f_p/f_s$]

subscripts

f	fluid
n	nanofluid flow
o	non-winglet
w	wall

CONFLICTS OF INTEREST

No conflict of interest was declared by the author.

REFERENCES

[1] Lei, Y. G., He, Y. L., Li, R., Gao, Y. F., "Effects of baffle inclination angle on flow and heat transfer of a heat exchanger with helical baffles", Chemical Engineering Research, 47(12): 2336–2345, (2008).

[2] Li, Z., Gao, Y., "Numerical study of turbulent flow and heat transfer in cross corrugated triangular ducts with delta-shaped baffles", International Journal of Heat and Mass Transfer, 108: 658–670, (2017).

[3] Sriromreun, P., "Numerical study on heat transfer enhancement in a rectangular duct with incline shaped baffles", Chemical Engineering Transactions, 57: 1243–1248, (2017).

[4] Rashidi, S., Eskandarian, M., Mahian, O., Poncet, S., "Combination of nanofluid and inserts for heat transfer enhancement, Gaps and challenges", Journal of Thermal Analysis and Calorimetry, 135: 437–460, (2019).

[5] Alnak, D. E., "Thermohydraulic performance study of different square baffle angles in cross-corrugated channel", Journal of Energy Storage, 28: 101295, (2020).

[6] Chang, S.W., Cheng, T. H., "Thermal performance of channel flow with detached and attached pin-fins of hybrid shapes under inlet flow pulsation", International Journal of Heat and Mass Transfer, 164: 120554, (2021).

[7] Kumar, R., Goel, V., Kumar, A., "Investigation of heat transfer augmentation and friction factor in triangular duct solar air heater due to forward facing chamfered rectangular ribs: a CFD based analysis", Renewable Energy,115: 824–835, (2018).

[8] Nakhchi, M. E., "Experimental optimization of geometrical parameters on heat transfer and pressure drop inside sinusoidal wavy channels", Thermal Science and Engineering Progress, 9: 121–31, (2019).

[9] Hassanzadeh, R., Tokgoz, N., "Thermal-hydraulic characteristics of nanofluid flow in corrugated ducts", Journal of Engineering Thermophysics, 26(4): 498-513, (2017).

[10] Tokgoz, N., Tunay, T., Sahin, B., "Effect of corrugated channel phase shifts on flow structures and heat transfer rate", Experimental Thermal and Fluid Science, 99: 374-391, (2018).

[11] Tokgoz, N., "Experimental and numerical investigation of flow structure in a cylindrical corrugated channel", International Journal of Mechanical Sciences, 157: 787-801, (2019).

[12] Hassanzadeh, R., Tokgoz, N., "Analysis of heat and fluid flow between parallel plates by inserting triangular cross-section rods in the cross-stream plane", Applied Thermal Engineering, 160, 113981, (2019)

[13] Karwa, R., Maheshwari, B. K., "Heat transfer and friction in an asymmetrically heated rectangular duct with half and fully perforated baffles at different pitches", International Communications in Heat and Mass Transfer, 36: 264–268, (2009).

[14] Sureandhar, G., Srinivasan, G., Muthukumar, P., Senthilmurugan, S., "Performance analysis of arc rib fin embedded in a solar air heater", Thermal Science and Engineering Progress, 23: 100891, (2021).

[15] Sripattanapipat, S., Promvonge, P., "Numerical analysis of laminar heat transfer in a channel with diamond-shaped baffles", International Communications in Heat and Mass Transfer, 36(1): 32-38, (2009).

[16] Kwankaomeng, S., Promvonge, P., "Numerical prediction on laminar heat transfer in square duct with 30° angled baffle on one wall", International Communications in Heat and Mass Transfer, 37: 857-866, (2010).

[17] Menasria, F., Zedairia, M., Moummi, A., "Numerical study of thermohydraulic performance of solar air heater duct equipped with novel continuous rectangular baffles with high aspect ratio", Energy, 133: 593-608, (2017).

[18] Karabulut, K., "Heat transfer and pressure drop evaluation of different triangular baffle placement angles in cross-corrugated triangular channels", Thermal Science, 24: 355-365, (2020).

[19] Promvonge, P., Tamna, S., Pimsarn, M., Thianpong, C., "Thermal characterization in a circular tube fitted with inclined horseshoe baffles", Applied Thermal Engineering, 75: 1147–1155, (2015).

[20] Kumar, R., Kumar, A., Chauhan, R., Sethi, M., "Heat transfer enhancement in solar air channel with broken multiple V-type baffle", Case Studies in Thermal Engineering, 8: 187–197, (2016).

[21] Sahel, D., Ameur, H., Benzeguir, R., Kamla, Y., "Enhancement of heat transfer in a rectangular channel with perforated baffles", Applied Thermal Engineering, 101: 156–164, (2016).

[22] Menni, Y., Azzi, A., Chamkha, A. J., Harmand, S., "Analysis of fluid dynamics and heat transfer in a rectangular duct with staggered baffles", Journal of Applied and Computational Mechanics, 5(2): 231-248, (2019).

[23] Luan, N. T., Phu, N. M., "Thermohydraulic correlations and exergy analysis of a solar air heater duct with inclined baffles", Case Studies in Thermal Engineering, 21: 100672, (2020).

[24] Bensaci, C.E., Moummi, A., Sanchez de la Flor, F.J., Rodriguez Jara, E.A., Rincon-Casado, A., Ruiz-Pardo, A., "Numerical and experimental study of the heat transfer and hydraulic performance of solar air heaters with different baffle positions", Renewable Energy, 155: 1231–1244, (2020).

[25] Wang, D., Liu, J., Liu, Y., Wang, Y., Li, B., Liu, J., "Evaluation of the performance of an improved solar air heater with "S" shaped ribs with gap", Solar Energy, 195: 89–101, (2020).

[26] Skullong, S., Promvonge, P., Thianpong, C., Pimsarn, M., "Thermal performance in solar air heater channel with combined wavy-groove and perforated-delta wing vortex generators", Applied Thermal Engineering, 100: 611–620, (2016).

[27] Tang, S. Z., Wang, F. L., He, Y. L., Yu, Y., Tong, Z. X., "Parametric optimization of H-type finned tube with longitudinal vortex generators by response surface model and genetic algorithm", Applied Energy, 239: 908–918, (2019).

[28] Promvonge, P., Skullong, S., "Thermo-hydraulic performance in heat exchanger tube with V-shaped winglet vortex generator", Applied Thermal Engineering, 164: 114424, (2020).

[29] Sun, Z., Zhang, K., Li, W., Chen, Q., Zheng, N., "Investigations of the turbulent thermal-hydraulic performance in circular heat exchanger tubes with multiple rectangular winglet vortex generators", Applied Thermal Engineering, 168: 114838, (2020).

[30] Zheng, N., Yan, F., Zhang, K., Zhou, T., Sun, Z., "A review on single-phase convective heat transfer enhancement based on multi-longitudinal vortices in heat exchanger tubes", Applied Thermal Engineering, 164: 114475, (2020).

[31] Nakhchi, M.E., Hatami, M., Rahmati, M., "Experimental investigation of performance improvement of double-pipe heat exchangers with novel perforated elliptic turbulators", International Journal of Thermal Sciences, 168: 107057, (2021).

[32] Modi, J. A., Rathod, M. K., “Comparative study of heat transfer enhancement and pressure drop for fin-and-circular tube compact heat exchangers with sinusoidal wavy and elliptical curved rectangular winglet vortex generator”, International Journal of Heat and Mass Transfer, 141: 310-326, (2019).

[33] Promvonge, P., Promthaisong, P., Skullong, S., “Experimental and numerical heat transfer study of turbulent tube flow through discrete V-winglets”, International Journal of Heat and Mass Transfer, 151: 119351, (2020).

[34] Akcay, S., Akdag, U., “Parametric investigation of effect on heat transfer of pulsating flow of nanofluids in a tube using circular rings”, Pamukkale University, Journal of Engineering Sciences, 24(4): 597-604, (2018).

[35] Tokgoz, N., Alıc, E., Kaska, O., Aksoy, M.M., “The numerical study of heat transfer enhancement using Al_2O_3-water nanofluid in corrugated duct application”, Journal of Thermal Engineering, 4(3): 1984-1997, (2018).

[36] Akdag, U., Akcay, S., Demiral, D., “Heat transfer enhancement with laminar pulsating nanofluid flow in a wavy channel”, International Communications in Heat Mass Transfer, 59: 17–23, (2014).

[37] Akdag, U., Akcay, S., Demiral, D., “Heat transfer enhancement with nanofluids under laminar pulsating flow in a trapezoidal-corrugated channel”, Progress in Computational Fluid Dynamics, 17(5): 302-312, (2017).

[38] Akdag, U., Akcay, S., Demiral, D., “Heat transfer in a triangular wavy channel with CuO-water nanofluids under pulsating flow”, Thermal Science, 23(1): 191-205, (2019).

[39] Fazeli, H., Madani, S., Mashaei, P.R., “Nanofluid forced convection in entrance region of a baffled channel considering nanoparticle migration”, Applied Thermal Engineering, 106: 293–306, (2016).

[40] Karouei, S.H.H., Ajarostaghi, S.S.M., Bandpy, M.G., Fard, S.R.H., “Laminar heat transfer and fluid flow of two various hybrid nanofluids in a helical double pipe heat exchanger equipped with an innovative curved conical turbulator”, Journal of Thermal Analysis and Calorimetry, 143: 1455–1466, (2021).

[41] Manca, O., Nardini, S., Ricci, D., “A numerical study of nanofluid forced convection in ribbed channels”, Applied Thermal Engineering, 37: 280-297, (2012).

[42] Heshmati, A., Mohammed, H. A., Darus, A.N., “Mixed convection heat transfer of nanofluids over backward facing step having a slotted baffle”, Applied Mathematics and Computation, 240: 368–386, (2014).

[43] Huminic, G., Huminic, A., “Heat transfer and flow characteristics of conventional fluids and nanofluids in curved tubes: A review”, Renewable and Sustainable Energy Reviews, 58: 1327–1347, (2016).

[44] Menni, Y., Chamkha, A. J., Ghazvini, M., Ahmadi, M. H., Ameur, H., Issakhov, A., Inc, M., “Enhancement of the turbulent convective heat transfer in channels through the baffling technique and oil/multiwalled carbon nanotube nanofluids”, Numerical Heat Transfer, Part A: Applications, 79(4): 311-351, (2021).

[45] Qi, C., Wan, Y.L., Li, C.Y., Han, D.T., Rao, Z. H., “Experimental and numerical research on the flow and heat transfer characteristics of TiO_2-water nanofluids in a corrugated tube”, International Journal of Heat and Mass Transfer, 115: 1072–1084, (2017).

[46] Pordanjani, A. H., Aghakhani, S., Afrand, M., Mahmoudi, B., Mahian, O., Wongwises, S., "An updated review on application of nanofluids in heat exchangers for saving energy", Energy Conversion Management, 198: 111886, (2019).

[47] Mei, S., Qi, C., Luo, T., Zhai, X., Yan, Y., "Effects of magnetic field on thermo-hydraulic performance of Fe_3O_4-water nanofluids in a corrugated tube", International Journal of Heat and Mass Transfer, 128: 24–45, (2019).

[48] Kaood, A., Hassan, M.A., "Thermo-hydraulic performance of nanofluids flow in various internally corrugated tubes", Chemical Engineering & Processing: Process Intensification, 154: 08043, (2020).

[49] Tian, M.-W., Khorasani, S., Moria, H., Pourhedayat, S., Dizaji, H.S., "Profit and efficiency boost of triangular vortex-generators by novel techniques", International Journal of Heat and Mass Transfer, 156: 119842, (2020).

[50] Ajeel, R.K., Sopian, K., Zulkifli, R., "Thermal-hydraulic performance and design parameters in a curved-corrugated channel with L-shaped baffles and nanofluid", Journal of Energy Storage, 34: 101996, (2021).

[51] Karabulut, K., Buyruk, E., Kılınç, F., "Experimental investigation of the effect of nanofluid including graphene-oxide nanoparticles on convective heat transfer and pressure drop enhancement in a straight pipe", Engineer and Machinery, 59(690): 45-67, (2018).

[52] Karabulut, K., Buyruk, E., Kılınc, F., "Experimental research of convective heat transfer for graphene-oxide nanofluid in a straight circular tube", 8th International Advanced Technologies Symposium (IATS'17), 7: 1368-1376, Elazıg-Turkey, (2017).

[53] Karabulut, K., Buyruk, E., Kılınc, F., "Experimental and numerical investigation of convection heat transfer in a circular copper tube using graphene oxide nanofluid", Journal of the Brazilian Society of Mechanical Sciences and Engineering, 42: 230, (2020).

[54] Kılınc, F., Buyruk, E., Karabulut, K., "Experimental investigation of cooling performance with graphene based nano-fluids in a vehicle radiator", Heat and Mass Transfer, 56: 521-530, (2020).

[55] ANSYS Inc., ANSYS Fluent user guide & theory guide- Release 15.0. USA, (2015).

[56] Kakac, S., Pramuanjaroenkij, A., "Review of convective heat transfer enhancement with nanofluids", International Journal of Heat and Mass Transfer, 52: 3187–3196, (2009).

[57] Meyer, J.P., Abolarin, S.M., "Heat transfer and pressure drop in the transitional flow regime for a smooth circular tube with twisted tape inserts and a square-edged inlet", International Journal of Heat and Mass Transfer, 117: 11-29, (2018).